J|A|C|S
COMMUNICATIONS

Published on Web 10/19/2002

Component B Binding to the Soluble Methane Monooxygenase Hydroxylase by Saturation-Recovery EPR Spectroscopy of Spin-Labeled MMOB

Ryan MacArthur,[†] Matthew H. Sazinsky,[‡] Henriette Kühne,[†] Douglas A. Whittington,[‡] Stephen J. Lippard,*[,‡] and Gary W. Brudvig*[,†]

Department of Chemistry, Yale University, P.O. Box 208107, New Haven, Connecticut 06520-8107, and Department of Chemistry, Massachusetts Institute of Technology, Cambridge, Massachusetts 02139

Received August 2, 2002

Soluble methane monooxygenase (sMMO) is a multicomponent enzyme system present in methanotrophic bacteria that catalyzes the reaction of methane with dioxygen to form methanol. Two nonheme diiron (Fe_2) centers, housed in four-helix bundles of the α-subunits of the dimeric hydroxylase (MMOH) component, reductively activate dioxygen for insertion into the C−H bond of methane.[1] The required electrons are provided by MMOR, a reductase component that accepts reducing equivalents from NADH. A third protein, required to couple electron transfer from MMOR to MMOH with the production of methanol, is component B (MMOB).[2] This cofactorless 16 kDa regulatory protein associates with the hydroxylase α-subunit[3] and changes its spectroscopic properties.[4,5] Together with MMOR, it also alters the reduction potentials of the Fe_2 center.[6] The mechanism by which MMOB activates MMOH and, until now, the binding location have been unknown.

Using saturation-recovery EPR (SREPR) spectroscopy, we probed the characteristics of the Fe_2^{III} center in MMOH (H_{ox}) from *Methylococcus capsulatus* (Bath) upon MMOB binding by measuring the spin−lattice (T_1) relaxation of an EPR spin-label, [1-oxyl-2,2,5,5-tetramethyl-Δ3-pyrroline-3-methyl] methane thiosulfonate (MTSL), specifically placed on the unique residue Cys89. The dipole−dipole interaction between the Fe_2^{III} center and MTSL revealed by this method provides information about both the magnetic exchange coupling within the Fe_2 center and its distance to the spin label upon formation of the MMOB/MMOH complex. The magnitude of the T_1 relaxation enhancement places the MMOB spin label close (15 ± 4 Å) to one of the Fe_2 centers in the MMOH dimer. This distance measurement provides the first direct physical evidence that MMOB binds in the canyon region[7] of the MMOH dimer interface adjacent to iron-coordinating helices E and F of the α-subunit.

When component B is modified by MTSL, the relaxation rate of the slow-relaxing spin label is significantly enhanced by the Fe_2 center of MMOH in the MMOB/MMOH complex. The enhancement of the MTSL SREPR recovery rate depends on the availability of such T_1 relaxation pathways. MMOB binding also affects the EPR spectrum of the Fe_2 center in the $Fe^{II}Fe^{III}$ mixed-valent state (H_{mv}). The $g_{av} < 2$ rhombic signal is broadened and shifted to higher field, indicating complex formation.[4,8] Since H_{ox} is difficult to quantify by EPR spectroscopy and has different magnetic properties than H_{mv}, conditions that maximized the MMOB/H_{mv} signal were used for H_{ox} samples. Broadening of the MTSL EPR signal at room temperature (Figure 1, inset), from slower motion of the spin label in the MMOB/MMOH complex, also served to optimize the sample conditions that maximized formation of the complex.

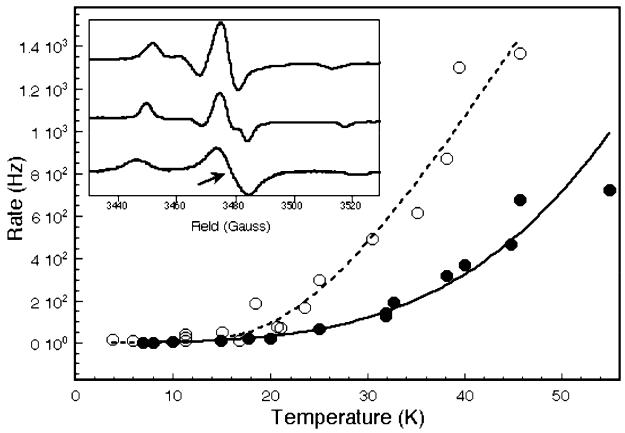

Figure 1. Temperature dependence of the T_1 relaxation rates of the MTSL spin-label in MMOB−MTSL (k_i, closed circles) and in the MMOB−MTSL/MMOH complex (k_d, open circles). The values of k_1 for the MMOB−MTSL samples were obtained from single-exponential fits of saturation-recovery EPR data. The values of k_d for the MTSL−MMOB/H_{ox} complex were obtained from fits of a dipolar relaxation model to saturation-recovery EPR data,[9−11] as described in the Supporting Information. The dashed line is a fit based on the relaxation enhancement from the Fe_2^{III} center, and the solid line is a power law fit for a noninteracting spin. Inset: CW EPR spectra of 80 μM MTSL−MMOB in 25 mM pH 7 MOPS, 25% glycerol (top), an identical sample in the presence of 80 μM MMOH (middle), and the latter in frozen solution (bottom). The arrow indicates the field position for SREPR traces. Conditions for room-temperature CW EPR spectra (inset, top and middle): modulation frequency, 100 kHz; modulation amplitude, 2.5 G; microwave frequency, 9.79 GHz; microwave power, 20.4 mW; temperature, 298 K. Conditions for low-temperature CW EPR spectrum (inset, bottom): modulation frequency, 100 kHz; modulation amplitude, 4 G; microwave frequency, 9.24 GHz; microwave power, 0.05 mW; temperature, 20 K. The bottom scan is scaled along the magnetic field axis to compensate for the difference in microwave frequencies.

SREPR traces from MTSL−MMOB samples alone are reasonably well fit by a single-component T_1 relaxation mechanism with a rate constant (k_i) as expected for an isolated spin.[12] In the MTSL−MMOB/H_{ox} complex, SREPR data require the addition of a second rate constant (k_d) to account for the dipolar interaction of MTSL with the Fe_2^{III} center of H_{ox}.[9−11] Relaxation enhancement of the MTSL−MMOB signal by H_{ox} is apparent from a plot of the relaxation rates from both types of samples (Figure 1). The ground spin state of the Fe_2^{III} center is diamagnetic owing to antiferromagnetic spin exchange coupling. Values for k_d of MTSL−MMOB/H_{ox} extracted from SREPR transients over a range of temperatures illustrate the T_1 relaxation enhancement of MTSL as higher paramagnetic spin states of H_{ox} become populated. The exchange coupling constant, $J_{ex}(Fe_2^{III})$, is estimated from $k_d(T)$ to be $-37 \pm$

* To whom correspondence should be addressed. E-mail: lippard@lippard.mit.edu, gary.brudvig@yale.edu.
[†] Yale University.
[‡] M.I.T.

10.1021/ja0279904 CCC: $22.00

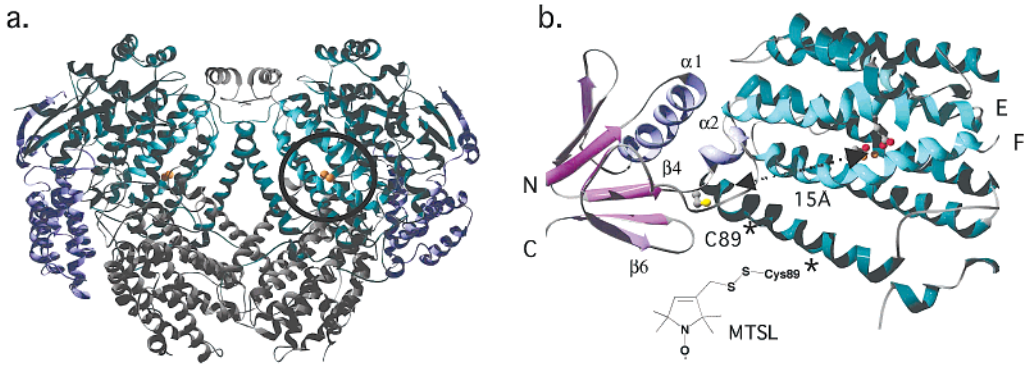

Figure 2. Proposed MMOH and MMOB binding surfaces. (a) Structure of MMOH depicting the canyon (dimer interface), helixes E and F (aqua), the proposed region of MMOB docking (black circle), and the diiron center (orange spheres). (b) Stucture of MMOB (left) and surface of the α-subunit. MTSL-labeled Cys89 and iron-coordinating residues Glu 209 (helix E) and Glu 243 (helix F) are depicted (ball-and-stick). The figures were made by using Swiss-Pdb Viewer.[13] The inset depicts the structure of an MTSL-modified cysteine residue.

3 cm^{-1}, which is similar to the value reported for radiolyticlly generated H_{mv} without MMOB.[14] This behavior may be contrasted with that of H_{mv} from *M. trichosporium* OB3b, which exhibits decreased exchange coupling, from −30 to −5 cm^{-1}, upon MMOB binding.[3]

Using the method of Gorun and Lippard[15] and the measured exchange coupling constant, we estimate the average shortest Fe−O bond length to be 1.89 Å. From existing crystal structures,[16] we calculate $J_{ex}(Fe_2^{III})$ for H_{ox} alone to be −2.6 cm^{-1} to −5.3 cm^{-1}, depending on the protomer used. Thus, binding of MMOB changes the character of the Fe_2^{III} center by shortening the metal−metal distance and increasing the magnetic coupling.

A possible structural explanation for the greater coupling upon MMOB binding is that the mobile Glu243 residue might supply an additional spin exchange pathway by contributing a single-atom bridge, as in reduced MMOH.[16] Alternatively, semibridging Glu144, could shorten its longer Fe−O bond or a bridging hydroxide could deprotonate to form μ-oxo bonds.

On the basis of a comparison to the SREPR data of the tyrosyl radical of the RNR-R2[10] and after accounting for relaxation afforded by exchange coupling in this protein, we estimate a dipolar distance of 15 ± 4 Å between the Fe_2^{III} center and the spin label bound to MMOB. In a previous study of RNR-R2,[9] we compared point dipole and distributed dipole models for the diiron center interacting with a tyrosyl radical (8.3 Å center-to-center distance). Inclusion of the distributed dipoles yielded a change of ∼10% in r versus the point dipole approximation, which is within our estimated errors. The 15 Å distance suggests only one possible binding surface on each face of the hydroxylase, namely the canyon region at the dimer interface (Figure 2).[7] Owing to the r^{-6} distance dependence of the dipolar interaction, only one of the two Fe_2 centers will dominate the relaxation enhancement. In particular, our distance requires that at most one α-helix, probably helix E or F of the MMOH α-subunit, be positioned between MTSL and the Fe_2^{III} center (Figure 2a). Both E and F contain residues, Glu209 and Glu243, respectively, that bind the iron atom (Fe2) having ligation geometry that varies with the oxidation state of the center. This analysis amplifies existing structural information about MMOB/MMOH binding from NMR spectroscopy.[17] Resonances from residues adjacent to Cys89, located on strand β_4 and helix α_2, are broadened when MMOB interacts with MMOH. Thus, it is likely that the turn in which the Cys89 is located is associated with the binding surface, with strand β_4 pointing in toward, and with helix α_2 flush against, the MMOH surface (Figure 2b).

In summary, MMOB binding alters the exchange coupling of the Fe_2 center in MMOH. These results, together with the determination of the distance between MTSL-modified Cys89 and the Fe_2^{III} center using SREPR spectroscopy, provide strong evidence that MMOB directly binds to the helices that contribute geometrically variable ligands to the Fe2 coordination sphere.

Acknowledgment. This work was supported by NIH Grants GM32134 (S.J.L.) and GM36442 (G.W.B.). M.H.S. was an NIH Biotechnology Grant trainee.

Supporting Information Available: Sample preparation, data analysis (theory and procedure), RNR k_d data, representative SREPR traces and fits, CW EPR spectra of $MMOH_{mv}$ ± MMOB, and *T*-dependence of single-exponential fits to MMO samples (PDF). This material is available free of charge via the Internet at http://pubs.acs.org.

References

(1) Merkx, M.; Kopp, D. A.; Sazinsky, M. H.; Blazyk, J. L.; Müller, J.; Lippard, S. J. *Angew. Chem., Int. Ed.* **2001**, *40*, 2782−2807.
(2) Gassner, G. T.; Lippard, S. J. *Biochemistry* **1999**, *38*, 12768−12785.
(3) Fox, B. G.; Liu, Y.; Dege, J. E.; Lipscomb, J. D. *J. Biol. Chem.* **1991**, *266*, 540−550.
(4) Davydov, R.; Valentine, A. M.; Komar-Panicucci, S.; Hoffman, B. M.; Lippard, S. J. *Biochemistry* **1999**, *38*, 4188−4197.
(5) Pulver, S.; Froland, W. A.; Fox, B. G.; Lipscomb, J. D.; Solomon, E. I. *J. Am. Chem. Soc.* **1993**, *115*, 12409−12422.
(6) (a) Liu, K. E.; Lippard, S. J. *J. Biol. Chem.* **1991**, *266*, 12836−12839; 24859. (b) Paulsen, K. E.; Liu, Y.; Fox, B. G.; Lipscomb, J. D.; Münck, E.; Stankovich, M. T. *Biochemistry* **1994**, *33*, 713−722. (c) Kazlauskaite, J.; Hill, H. A. O.; Wilkins, P. C.; Dalton, H. *Eur. J. Biochem.* **1996**, *241*, 552−556.
(7) Rosenzweig, A. C.; Frederick, C. A.; Lippard, S. J.; Nordlund, P. *Nature* **1993**, *366*, 537−543.
(8) Fox, B. G.; Hendrich, M. P.; Surerus, K. K.; Andersson, K. K.; Froland, W. A.; Lipscomb, J. D.; Münck, E. *J. Am. Chem. Soc.* **1993**, *115*, 3688−3701.
(9) Galli, C.; Atta, M.; Andersson, K.; Gräslund, A.; Brudvig, G. W. *J. Am. Chem. Soc.* **1995**, *117*, 740−746.
(10) Hirsh, D. J.; Beck, W. F.; Lynch, J. B.; Que, L., Jr.; Brudvig, G. W. *J. Am. Chem. Soc.* **1992**, *114*, 7475−7481.
(11) Rakowsky, M. H.; More, K. M.; Kulikov, A. V.; Eaton, G. R.; Eaton, S. S. *J. Am. Chem. Soc.* **1995**, *117*, 2049−2057.
(12) Beck, W. F.; Innes, J. B.; Lynch, J. B.; Brudvig, G. W. *J. Magn. Reson.* **1991**, *91*, 12−29.
(13) Guex, N.; Peitsch, M. C. *Electrophoresis* **1997**, *18*, 2714−2723. http://www.expasy.ch/.
(14) DeWitt, J. G.; Bentsen, J. G.; Rosenzweig, A. C.; Hedman, B.; Green, J.; Pilkington, S.; Papaefthymiou, G. C.; Dalton, H.; Hodgson, K. O.; Lippard, S. J. *J. Am. Chem. Soc.* **1991**, *113*, 9219−9235.
(15) Gorun, S. M.; Lippard, S. J. *Inorg. Chem.* **1991**, *30*, 1625−1630.
(16) (a) Rosenzweig, A. C.; Nordlund, P.; Takahara, P. M.; Frederick, C. A.; Lippard, S. J. *Chem. Biol.* **1995**, *2*, 409−418. (b) Whittington, D. A.; Lippard, S. J. *J. Am. Chem. Soc.* **2001**, *123*, 827−838.
(17) (a) Walters, K. J.; Gassner, G. T.; Lippard, S. J.; Wagner, G. *Proc. Natl. Acad. Sci. U.S.A.* **1999**, *96*, 7877−7882. (b) Chang, S.-L.; Wallar, B. J.; Lipscomb, J. D.; Mayo, K. O. *Biochemistry* **2001**, *40*, 9539−9551.

JA0279904